GLUT2 Accumulation in Enterocyte Apical and Intracellular Membranes

A Study in Morbidly Obese Human Subjects and *ob/ob* and High Fat–Fed Mice

Amal Ait-Omar,[1] Milena Monteiro-Sepulveda,[1] Christine Poitou,[2,3] Maude Le Gall,[1] Aurélie Cotillard,[2] Jules Gilet,[1] Kevin Garbin,[1] Anne Houllier,[1] Danièle Château,[1] Amélie Lacombe,[4] Nicolas Veyrie,[2,5] Danielle Hugol,[6] Joan Tordjman,[2] Christophe Magnan,[4] Patricia Serradas,[1] Karine Clément,[2,3] Armelle Leturque,[1] and Edith Brot-Laroche[1]

OBJECTIVE—In healthy rodents, intestinal sugar absorption in response to sugar-rich meals and insulin is regulated by GLUT2 in enterocyte plasma membranes. Loss of insulin action maintains apical GLUT2 location. In human enterocytes, apical GLUT2 location has not been reported but may be revealed under conditions of insulin resistance.

RESEARCH DESIGN AND METHODS—Subcellular location of GLUT2 in jejunal enterocytes was analyzed by confocal and electron microscopy imaging and Western blot in 62 well-phenotyped morbidly obese subjects and 7 lean human subjects. GLUT2 locations were assayed in *ob/ob* and *ob/+* mice receiving oral metformin or in high-fat low-carbohydrate diet–fed C57Bl/6 mice. Glucose absorption and secretion were respectively estimated by oral glucose tolerance test and secretion of [U-^{14}C]-3-*O*-methyl glucose into lumen.

RESULTS—In human enterocytes, GLUT2 was consistently located in basolateral membranes. Apical GLUT2 location was absent in lean subjects but was observed in 76% of obese subjects and correlated with insulin resistance and glycemia. In addition, intracellular accumulation of GLUT2 with early endosome antigen 1 (EEA1) was associated with reduced MGAT4a activity (glycosylation) in 39% of obese subjects on a low-carbohydrate/high-fat diet. Mice on a low-carbohydrate/high-fat diet for 12 months also exhibited endosomal GLUT2 accumulation and reduced glucose absorption. In *ob/ob* mice, metformin promoted apical GLUT2 and improved glucose homeostasis. Apical GLUT2 in fasting hyperglycemic *ob/ob* mice tripled glucose release into intestinal lumen.

CONCLUSIONS—In morbidly obese insulin-resistant subjects, GLUT2 was accumulated in apical and/or endosomal membranes of enterocytes. Functionally, apical GLUT2 favored and endosomal GLUT2 reduced glucose transepithelial exchanges. Thus, altered GLUT2 locations in enterocytes are a sign of intestinal adaptations to human metabolic pathology. ***Diabetes*** **60:2598–2607, 2011**

The intestinal tract is determinant in energy homeostasis through control of sugar absorption and gut hormone release during digestion (1–4). Accordingly, the regulation of nutrient absorption has implications in metabolic diseases and their increasing prevalence worldwide.

Sugar absorption relies on the coordinated functions of transporters at the surface membrane of enterocytes. In the apical plasma membrane, the high-affinity Na-coupled cotransporter SGLT1 performs glucose and galactose extraction from the lumen (2) and GLUT5 transports dietary fructose (5). In the basolateral membrane, GLUT2 provides an exit pathway (6,7). These transporters are expressed in the duodenum and jejunum and at lower levels in the ileum. In rodent intestine, GLUT7, a high affinity transporter for glucose and fructose, was identified in the apical membranes of ileal enterocytes and colonocytes (8). Rodent models have shown that GLUT2 can be inserted into enterocyte apical membranes in response to oral glucose or fructose (9,10). This result constitutes an adaptation process to complement SGLT1 and GLUT5 uptake capacities when dietary sugar intake is high (10). Apical GLUT2 translocation is linked to dietary sugar concentration in the lumen and is reduced by fasting (10,11). Apical GLUT2 has been identified in adult and neonate rodent enterocytes as well as in insects, sheep, and pigs (rev. in 12,13). Although different signaling mechanisms have been reported to promote insertion of GLUT2 into apical membranes of enterocytes (rev. in 12), only insulin has been shown to trigger GLUT2 internalization, thereby slowing sugar uptake in the intestine during digestion (14). The relevance of this mechanism in the human small intestine deserves investigation. However, GLUT2 trafficking in human enterocytes is supported by studies in enterocytic Caco-2/TC7 cells (14,15). Ethical considerations render it difficult to directly study the impact of sugar on enterocyte GLUT2 location in humans.

In mice, insulin resistance maintains GLUT2 in enterocyte apical membranes, thereby creating conditions for increased dietary sugar uptake (14). Furthermore, experimental diabetes in rats with insulinopenia and hyperglycemia

From [1]INSERM, U872, Team 9, Paris, France; Centre de Recherche des Cordeliers, Université Pierre et Marie Curie-Paris 6, UMR S 872, Paris, France; [2]INSERM, U872, Team 7 Nutriomique, Paris, France; Centre de Recherche des Cordeliers, Université Pierre et Marie Curie-Paris 6, UMR S 872, Paris, France; the [3]Nutrition and Endocrinology Department, Assistance Publique-Hôpitaux de Paris, Pitié-Salpêtrière Hospital, Paris, France; Centre Recherche en Nutrition Humaine (CRNH) Ile de France, Paris, France; the [4]Centre National de la Recherche Scientifique (EAC4413), Université Paris-Diderot, Paris, France; the [5]Surgery Department, Assistance Publique-Hôpitaux de Paris, Hôtel-Dieu Hospital, Paris, France; and the [6]Pathology Department, Assistance Publique-Hôpitaux de Paris, Hôtel-Dieu Hospital, Paris, France.

Corresponding author: Edith Brot-Laroche, edith.brot-laroche@crc.jussieu.fr.

Received 15 December 2010 and accepted 31 July 2011.

DOI: 10.2337/db10-1740

This article contains Supplementary Data online at http://diabetes.diabetesjournals.org/lookup/suppl/doi:10.2337/db10-1740/-/DC1.

A.A.-O., M.M.-S., and C.P. contributed equally to this work.

provokes mucosal hypertrophy and increases mRNA and protein expression of GLUT2, GLUT5, and SGLT1 (16). In humans, obesity is characterized by the development of insulin resistance and type 2 diabetes (17–20). However, apical GLUT2 was not found in duodenal biopsies of overweight human type 2 diabetic subjects (21).

Insulin sensitizers are used in the treatment of type 2 diabetic subjects. In rodents, metformin increases intestinal sugar use (22,23) and expression of SGLT1 and GLUT5 (24) and it decreases glucose absorption (25). Metformin also promotes apical GLUT2 location in rodent enterocytes via AMP-activated protein kinase (AMPK) (26). In the human intestine, the effects of metformin on GLUT2 location have not yet been reported.

Bariatric surgery is a therapeutic option to reduce obesity with a curative potential for severe metabolic disorders (27). In jejunal samples obtained during bypass surgery of morbidly obese subjects, changes in GLUT2 location in enterocytes are expected according to the metabolic status of subjects. In the current study, morbidly obese subjects were carefully characterized for history of obesity, comorbidities, treatments, and dietary composition from questionnaires. GLUT2 location in jejunal enterocytes of obese and lean control subjects was assayed, and links with bioclinical parameters were analyzed. The consequences of insulin resistance, diabetes and dietary habits on intestinal function were revealed from comparison with lean subjects. The impact of metformin treatment and high-fat diet on GLUT2 distribution were explored in genetically obese and wild-type mice, respectively.

RESEARCH DESIGN AND METHODS

Human obese and lean subjects. Morbidly obese subjects (n = 62) involved in a gastric surgery program were recruited (2006–2008) in the Nutrition Department, CRMO, Hôtel-Dieu Hospital, Paris, France. Subjects (n = 14 for men; n = 48 for women) were aged between 19 and 64 years and met criteria for bariatric surgery: BMI ≥40 kg/m^2 (90%) or BMI ≥35 kg/m^2 combined with at least one comorbidity (type 2 diabetes, hypertension, obstructive apnea syndrome, or dyslipidemia). On the basis of the dietary food questionnaires, subjects could be defined as high-fat eaters when ingesting >30% of calories as lipid and low-carbohydrate eaters when ingesting <50% of calories as carbohydrate. Lean subjects (n = 7) were selected from a set of age-paired (range 17–68 years) normal-weight nondiabetic individuals. Subjects were fasted as required for the surgery.

Jejunal samples of obese and lean subjects. A tissue bank was made with jejunal samples usually discarded during Roux-en-Y gastric bypass. Samples were fixed in alcohol-formalin-acetic acid (AFA) after excision and imbedded in paraffin wax by pathologists. Some samples were snap-frozen in liquid nitrogen for biochemical investigations. Jejunal biopsies taken during routine gut exploration of seven lean subjects were obtained by double-balloon explorative enteroscopy and sent to the pathology department.

Obesity and insulin resistance in mice. Severe insulin resistance without obesity was induced in C57Bl/6 mice by feeding a high-fat low-carbohydrate diet (HFLC) (5,623 cal/kg, 72% fat [corn oil and lard], 28% protein, and <1% carbohydrate; SAFE, Augy, France) for 12 months starting at weaning (28). Control mice were fed an M25 diet (3,130 cal/kg, 3% fat, 23% protein, 51% carbohydrate; SAFE, Augy, France) (14).

Genetically obese *ob*/*ob* mice and wild-type *ob*/+ littermates (10 weeks; Janvier, Le Genest Saint Isle, France) were fed the M25 control diet and given 25 mg/kg metformin or H_2O per os at 9:00 A.M. and 6:00 P.M. for 10 days. Tail-blood glucose concentration (Accu-Check; Roche Diagnostics GmbH, Mannheim, Germany) and plasma insulin levels (enzyme immunosorbent assay [EIA]; Linco/Millipore, Guyancourt, France) were measured during an oral glucose tolerance test (OGTT) (4 g/kg) and after an 18-h fast (14). Homeostasis model assessment–insulin resistance (HOMA-IR) values were calculated (29) before and after treatment with metformin.

Immunofluorescence and confocal microscopy. Immunofluorescence staining was performed on 7-μm tissue sections (14) and analyzed by confocal microscopy (LSM710, Zeiss, Germany; 63× oil lens, 0.8 μm depth of field) for samples from 62 obese and 7 lean subjects. Three specific tailor-made GLUT2 antibodies were used to locate hGLUT2, including antibodies targeting the COOH-terminal (rat hGLUT2^{Cter}; Eurogentec, Angers, France) and the first extracellular X-loop1 (rabbit hGLUT2$^{X\text{-}loop1\text{-}GWG}$; GW Gould, Glasgow, Scotland) and hmrGLUT2$^{X\text{-}loop1\text{-}GLK}$ (GL Kellett, York, U.K.) (10,30). The latter two antibodies gave identical results, and hmrGLUT2$^{X\text{-}loop1\text{-}GLK}$ gave no signal in GLUT2$^{-/-}$ mice (10). COOH-terminal and X-loop1 GLUT2 antibodies were added sequentially at 1/500 dilutions after citrate unmasking (95°C, 10 min). Cell membrane markers, Na,KATPase (basolateral, Abcam mAb2871, 1/500), early endosome antigen 1 (EEA1) (goat-SC6415, 1/500; Santa Cruz Biotechnology, Santa Cruz, CA), protein disulfide isomerase (PDI) (rough endoplamic reticulum [RER], BD Biosciences, m610946, 1/250), GRP78/BIP (RER, BD Biosciences, San Diego, CA, rab610978, 1/250), Lamp1 (Lysosomes, mCD107a, BD Biosciences, 1/500), and MGAT4a antibody (glycosyl transferase antibody, ab56971 Abcam, Cambridge, U.K., 1/250) were used as membrane markers and to monitor glycosylation activity. In mouse studies, hmrGLUT2$^{\times\text{-}loop1\text{-}GLK}$ antibody was used after deglycosylation with *N*-glycosidase F (150 units/L; Roche Diagnostics, Mannheim, Germany) (30). Primary antibodies were revealed with rat, rabbit, goat, or mouse secondary antibodies coupled with cyanin (Jackson ImmunoResearch Laboratories, Newmarket, Suffolk, U.K., 1/1,000) or Alexa Fluor (1/400).

Immunoelectron microscopy. Eight jejunal samples were fixed with 4% paraformaldehyde (PFA) and 0.1% glutaraldehyde after dissection. After alcohol-graded dehydration, embedding in polyhydroxy-aromatic acrylic LR-White resin, ultra-thin sections were incubated with hGLUT2$^{X\text{-}loop1\text{-}GWG}$ antibody (1/500) followed by 12 nm gold particle-donkey anti-rabbit IgGs (Jackson ImmunoResearch Laboratories, Newmarket, Suffolk, UK). Sections were analyzed in a Jeol 100 CX II electron microscope coupled with an Erlangshen 1000 camera and software (Gatan; Roper Scientific, Evry, France).

Biochemical analysis of GLUT2 location. Apical membrane purification from frozen jejuna (n = 6) was performed ($MgCl_2$/EGTA method [31]) after a 45-s homogenization (FastPrepR-24; MP Biomedicals, Montreal, Canada) maintaining 1% antiprotease (Roche Diagnostics, Mannheim, Germany) and ice-cold conditions. Membrane density gradients (30–10% iodixanol; Optiprep, St. Louis, MO) were performed as previously described (14), with 2 mg postnuclear membranes from frozen jejuna (n = 4). Nineteen fractions (500 μL) were analyzed by Western blot (75 μL). Signals were quantified (LAS-4000 Imager, Fuji Film, GE Healthcare), and fraction densities were normalized to total signal. Sucrase activity (31) revealed apical membranes, and the Na, KATPase antibody revealed the basolateral membranes. Use of H-67 (SC-9117; Santa Cruz Biotechnology, Inc., Santa Cruz, CA), hGLUT2$^{X\text{-}loop1\text{-}GWG}$, or hGLUT2^{Cter} antibodies gave identical results.

In vivo estimation of glucose fluxes through jejunal mucosa in obese and lean mice. Glucose absorption was estimated by the rate of increase of blood glucose concentration (T15/T0 min) during OGTT (4 g/kg) in freely moving mice. Glucose efflux from the intestine was estimated by [U-^{14}C]-3-*O*-methyl glucose (3-OMG) accumulation for 30 min in the intestinal lumen of *ob*/*ob* and *ob*/+ mice. Catheters were implanted in right jugular veins, filled with heparin (10 units/mL), and flushed for 5–7 days during recovery from surgery. Mice were fasted overnight. Tail blood glucose concentration was monitored (glucose analyzer; LifeScan, CA) after intraperitoneal injection of glucose (1 g/kg), reaching a plasma concentration of 25.5 ± 5.0 and 6.6 ± 1.2 mmol/L after 30 min in *ob*/*ob* and *ob*/+ mice, respectively. Mice simultaneously received an oral bolus of 0.3/1.0 mmol/L cytochalasin B/phloretin or vehicle (gavage) and a vascular injection of [U-^{14}C]-3-OMG (2 μCi). [U-^{14}C]-3-OMG was counted (Aqualuma Plus, Lumac, The Netherlands; Packard Tri-Carb 460C counter) in 10 μL deproteinized blood [$Ba(OH)_2$/$ZnSO_4$]. Luminal contents were flushed with 500 μL saline and centrifuged (1,000*g*, 2 min, 4°C) to discard cells and solid content. Radioactivity in luminal fluid was expressed (μg · kg^{-1} · min^{-1} ± SEM) using blood glucose–specific activity as a reference.

Ethics statement. The Ethics Committee of Hôtel-Dieu Hospital approved the clinical investigations for both obese and lean subjects who gave written informed consent. Experiments with mice received approbation by the local ethics committee of Université Pierre et Marie Curie (UPMC) for animal use (p3/2008/042).

Statistical analysis. Results are expressed as mean ± SEM, and the significance between the mean of continuous parameters was evaluated by the Mann-Whitney statistical test using the StatEL or R statistics software packages (http://www.r-project.org). Contingency tables were performed for analysis of categorical data. The χ^2 statistics tests (or Fisher exact test for small sample size) were used to test the independence of GLUT2 localization and the other categorical data. All probabilities were two-tailed with significance set at $P < 0.05$.

RESULTS

Phenotype of morbidly obese human subjects. Preoperative evaluation is described in Table 1 and includes detailed medical history, body composition, and metabolic, nutritional (food quantity, macronutrient composition from

TABLE 1
Bioclinical parameters of morbidly obese subjects

	Nondiabetic obese subjects	Diabetic obese subjects
n	28	34
Age of surgery (years)	40 ± 2	49 ± 2*
Diabetes duration (years)		7.9 ± 1.3
Weight (kg)	135 ± 5	135 ± 4
BMI (kg/m^2)	50 ± 2	48 ± 1
Age of diabetes start (years)		42 ± 2
Insulin (mU/L)	13 ± 1	17 ± 3
Blood glucose (mmol/L)	5.3 ± 0.2	8.7 ± 0.6†
HOMA-IR	3.1 ± 0.4	5.2 ± 0.9*
HbA_{1c} (%)	5.6 ± 0.1	7.7 ± 0.3†
C-reactive protein (mg/L)	9.6 ± 1.4	9.4 ± 1.4
Total cholesterol (mmol/L)	4.8 ± 0.2	4.5 ± 0.2
HDL cholesterol (mmol/L)	1.4 ± 0.1	1.3 ± 0.1
Triglycerides (mmol/L)	1.3 ± 0.1	1.8 ± 0.2*
Total calorie intake (kcal/day)	2,073 ± 115	2,102 ± 104
Proteins (%)	18 ± 1	19 ± 1
Lipids (%)	36 ± 1	35 ± 1
Carbohydrates (%)	45 ± 1	46 ± 2

Data are means ± SEM. Insulin was measured by immunoradiometric assay. Mean HOMA-IR values were calculated in 41 subjects using the formula [glucose (mmol/L) × insulin (mU/L)/22.5] (http://www.dtu.ox.ac.uk), excluding insulin- and/or sulfamid-treated subjects. Mann-Whitney *U* or Fisher exact tests were performed to compare nondiabetic and diabetic subjects. *$P < 0.01$. †$P < 0.001$.

detailed questionnaire by dietitian), cardiopulmonary, and psychological assessments. Obese subjects did not demonstrate any evidence of acute or chronic systemic inflammation (C-reactive protein), infectious disease, viral infection, cancer, or known alcohol consumption (>20 g/day). HOMA-IR taken as an index of insulin resistance was over 1.75 in 92% of obese subjects, excluding patients with exogenous insulin treatment. Obese subjects were defined as diabetic by fasting blood glucose over 7 mmol/L ($n = 34$) and by prescription of antidiabetic treatment ($n = 27$). For the purposes of analysis, two groups of nondiabetic obese subjects were created using the median value of fasting blood glucose concentration (5.31 mmol/L), i.e., [glucose] <5.31 ($n = 14$), [glucose] ≥5.31 ($n = 14$), to be compared with untreated diabetic obese subjects ($n = 7$) (Supplementary Table 1). The treated diabetic obese subjects took a combination of oral medication with metformin (44%) or insulin (19%). The other subjects took combined insulin and metformin (30%) or oral medication alone (7%).

GLUT2 locations in enterocytes of lean and morbidly obese human subjects

Basolateral location of GLUT2. As expected in fasting subjects, GLUT2 was localized with Na,KATPase in basolateral membranes of enterocytes lining the villi, but was absent from immature crypt cells in both lean ($n = 7$; 100%) and obese ($n = 62$; 100%) subjects (Fig. 1*A* and Supplementary Fig. 1). We observed that 13% of obese subjects (three nondiabetic and five treated diabetic) exhibited basolateral membrane–only GLUT2 (Supplementary Fig. 1).

Apical and basolateral membrane locations of GLUT2. In addition to the basolateral membrane location, GLUT2 was detected in apical membranes of mature enterocytes from fasting obese subjects (Fig. 1*A*, *right*, and Supplementary Fig. 1). Purified apical membranes, which were devoid of Na,KATPase basolateral contamination, revealed GLUT2 and GLUT5 by Western blot analysis ($n = 6$, Fig. 1*B*). Enterocyte membrane separation on density gradients ($n = 4$, Fig. 1*C*) showed full-length GLUT2 protein cosegregated with apical marker sucrase (fractions 11–15) and basolateral marker Na,KATPase (fractions 7–10). Finally, electron microscopy images showed GLUT2-associated gold particles in apical and basolateral membranes ($n = 8$, Fig. 1*D*). These findings demonstrate the presence of GLUT2 in apical and basolateral membranes of obese human enterocytes.

Apical GLUT2 was significantly more frequent in jejunal enterocytes of obese subjects (76%) than in lean fasting subjects (0%; $P = 0.0002$). In obese subjects, apical GLUT2 was associated with increased total-calorie ($P = 0.002$) and carbohydrate ($P = 0.03$) intake (Supplementary Table 2). The occurrence of apical GLUT2 increased with fasting blood glucose concentrations (Fig. 1*E*, $R^2 = 0.99$) and HOMA-IR values ($R^2 = 0.99$), highlighting the link between apical GLUT2 and insulin resistance.

Most diabetic obese subjects took metformin (74%) or insulin (48%) in various combinations with other oral antidiabetic drugs (OADs). Although observed in a few subjects, 65% of metformin-treated diabetic obese subjects and all obese subjects taking insulin and metformin exhibited apical GLUT2 (Supplementary Table 3). However, the effects of metformin alone or in combination could not be established unequivocally, since only 18% of diabetic obese subjects received metformin as single antidiabetic therapy. *Ob/ob* mice were therefore used to assess the effects of metformin on GLUT2 location.

Endosomal accumulation of GLUT2 in enterocytes of morbidly obese subjects. GLUT2 accumulated above the nucleus of enterocytes (Fig. 2 and Supplementary Fig. 2) in 39% of obese subjects. Most of them (71%) also exhibited apical GLUT2. This intracellular GLUT2 colocalized with EEA1 (Fig. 2*A* and Supplementary Fig. 3*A*), but not with LAMP1 (late endosomes/lysosomes; Supplementary Fig. 3*B*) or with BIP/GPR78 (Supplementary Fig. 3*C*) or PDI (endoplasmic reticulum; Supplementary Fig. 3*D*). In contrast with basolateral and apical GLUT2 locations, this intracellular GLUT2 was found in villous and crypt cells (Supplementary Fig. 2) and was identified with two different antibodies targeting the extracellular loop1 and COOH-terminal antibodies (Supplementary Fig. 2), suggesting a trafficking default of full-length GLUT2 protein.

Glycosylation is a key element of protein trafficking. MGAT4a glycosyl transferase was reduced by twofold in enterocytes from obese subjects exhibiting endosomal GLUT2 accumulation above the nucleus versus apical GLUT2 (Fig. 2*B*). Thus, endosomal GLUT2 accumulation likely results from altered glycosylation processes.

The number of obese subjects exhibiting endosomal GLUT2 accumulation revealed a link with the macronutrient composition of their diet (Fig. 2*C*) but not with total calorie intake (Supplementary Table 2). Indeed, 83% of subjects exhibiting endosomal GLUT2 accumulation were high-fat eaters (*black columns*; $P = 0.04$) versus 55% of subjects with other GLUT2 locations. Endosomal GLUT2 accumulation was also related to lower carbohydrate consumption (*white columns*; $P = 0.04$). We next used a mouse model to test the hypothesis that unbalanced carbohydrate/high-fat diets could promote GLUT2 accumulation above the nucleus.

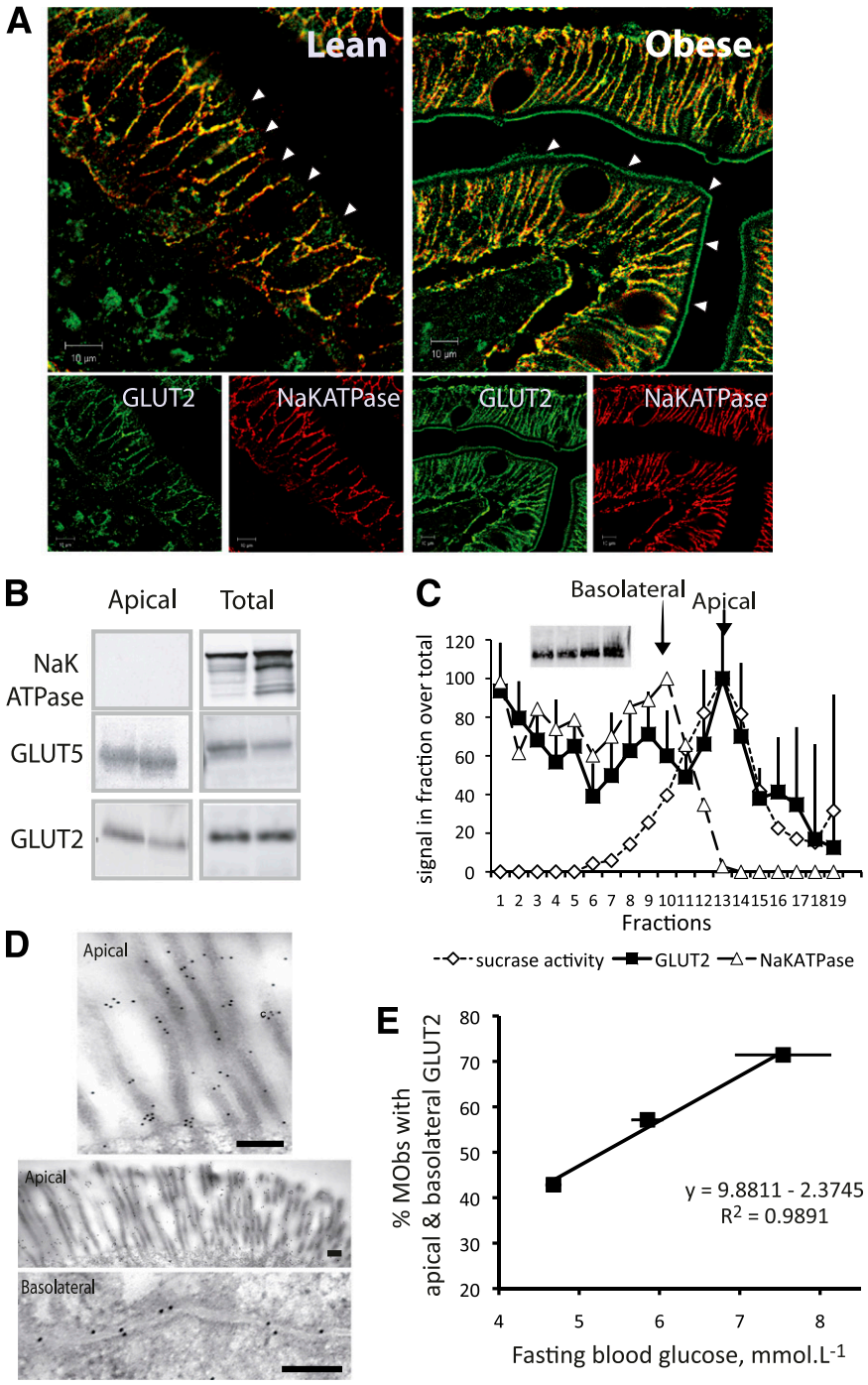

FIG. 1. Apical location of GLUT2 in enterocytes from jejunal samples of morbidly obese subjects (MObs). *A*: Representative confocal microscopy images of the location of GLUT2 (*green*) in apical membranes and in basolateral membranes colocalizing (*yellow*) with Na,KATPase (*red*). Images, representative of 30 obese (*right panel*) and 7 lean (*left panel*) subjects, were obtained with 2 antibodies targeting X-loop1 and COOH-terminal peptides of GLUT2 (Supplementary Fig. 1 for details). *Arrows* indicate apical membrane domains. Scale 10 μm. *B*: Two representative Western blots of Na,KATPase, GLUT5, and GLUT2 in purified apical and postnuclear membranes (total) from the jejuna of six obese subjects. *C*: Quantification of GLUT2 (■) in fractions (75/500 μL) obtained from the separation on density gradients of enterocyte membranes analyzed in Western blots. Na,KATPase (Western blot, *dashed line*, △) and sucrase activity (*dotted line*, ◇) were used to identify apical and basolateral membrane fractions, respectively. Insert shows a Western blot of GLUT2 inputs. Data represent the average densities obtained for four obese subjects (arbitrary units ± SEM). *D*: Immuno-gold electron microscopy images of GLUT2 in apical and basolateral membranes of enterocytes. Scale 0.2 μm. *E*: Linear regression analysis of the percentage of untreated obese subjects exhibiting apical GLUT2 as a function of mean fasting glycemia. Three subject groups were created using the median blood glucose concentration >5.3 or <5.3 mmol/L or in untreated diabetes (R^2 = 0.99). (A high-quality digital representation of this figure is available in the online issue.)

Impact of diet and metformin on GLUT2 location in the mouse enterocyte

Phenotype of HFLC-fed mice. Fasting insulin concentration increased threefold in HFLC-fed mice for 12 months (Table 2). In euglycemic-hyperinsulinemic clamp conditions, HFLC mice exhibited a ninefold lower glucose infusion rate after 5 months than controls, indicating severe insulin resistance (Table 2). Thus, HFLC mice provided a model of insulin resistance in lean mice.

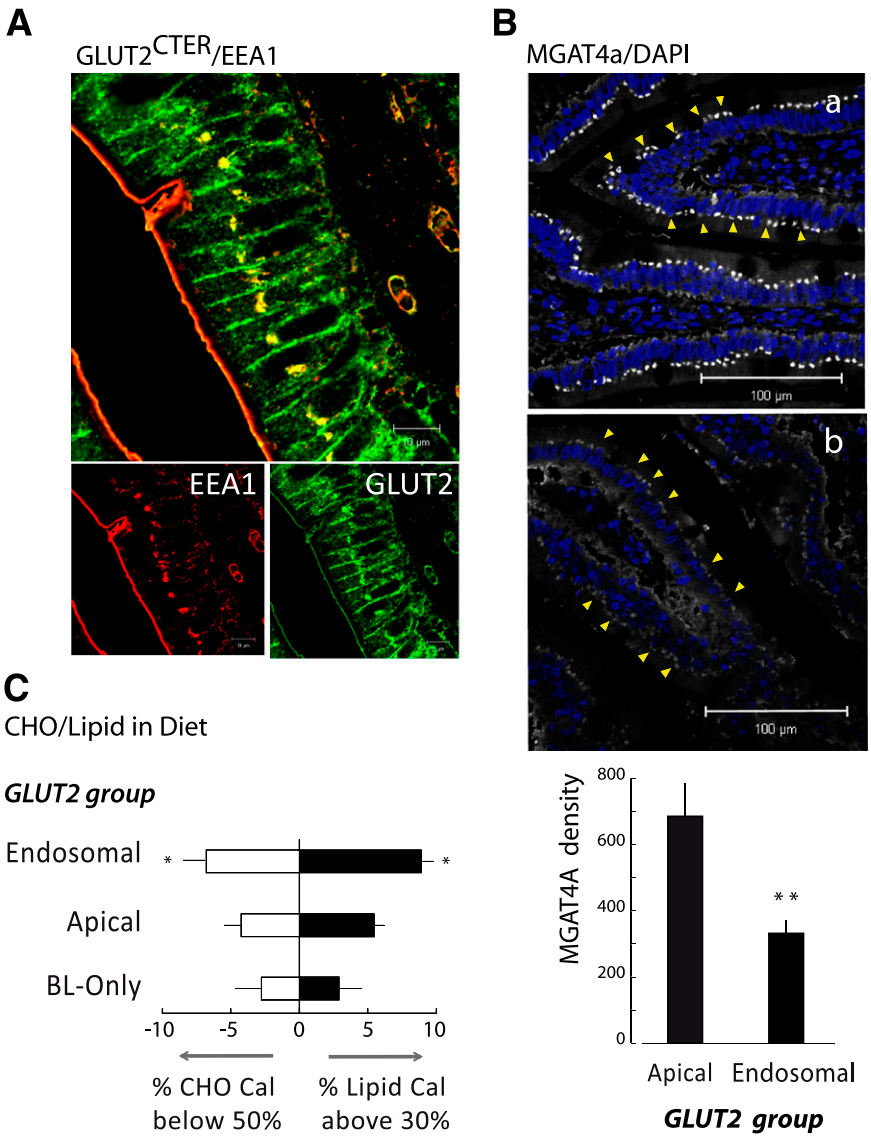

FIG. 2. Accumulation of GLUT2 in endosomes in jejunal enterocytes of obese subjects. *A*: Representative image of the colocation (*yellow*) of GLUT2 (*green*) with the endosome marker EEA1 (*red*). Confocal microscopy images were performed as in Fig. 1 (scale 10 µm). *B*: Representative images of MGAT4a glycosyltransferase protein expression comparing the jejuna of obese subjects with apical or endosomal GLUT2 accumulation. Immunolabeling and confocal image acquisitions were performed in parallel in apical (*a*, *n* = 10) and endosomal (*b*, *n* = 10) groups. *Yellow arrows* identify the location of MGAT4 in the enterocytes. Quantification of MGAT4a density in both types of subjects was measured with the ImageJ software (*P* < 0.0041). *C*: Carbohydrate (CHO) and lipid calories in diets of obese subjects grouped according to GLUT2 location, i.e., only in basolateral membrane (BL-only), in endosomal, or in apical membranes. Data represent the average deviation of calorie content ± SEM (>30% lipid calorie, ■; **P* < 0.038) or carbohydrate calorie (<50%, □; **P* < 0.043). (A high-quality digital representation of this figure is available in the online issue.)**

Endosomal GLUT2 accumulation in enterocytes of HFLC-fed mice. Mice fed an HFLC diet for 12 months were insulin resistant but had similar weight gain as control mice (M25 diet) (Table 2). OGTTs revealed the progress of glucose intolerance (Fig. 3*A*) and significant increase of fasting blood glucose concentration (Fig. 3*B*) with time of exposure to HFLC diet when compared with controls. As anticipated, GLUT2 was found in basolateral membranes in healthy control mice (Fig. 3*C*). In contrast, all HFLC mice exhibited endosomal accumulation and significantly lower levels of basolateral GLUT2 in enterocytes (Fig. 3*D*). These GLUT2 locations resemble those of obese subjects eating unbalanced fat/carbohydrate diets.

In HFLC mice, glucose absorption decreased slowly, as indicated by the significantly lower initial slope of blood glucose concentration during OGTT (Fig. 3*E*), i.e., basal glucose concentration increased (Fig. 3*B*) with essentially a similar 15-min glucose concentration in OGTT. As expected from a low-carbohydrate dietary supply, the protein abundance of GLUT2 in jejuna was reduced in HFLC-fed mice compared with control mice (Fig. 3*F*). Sequestration of GLUT2 in intracellular compartments and lower levels of GLUT2 expression could explain the lower rates of glucose absorption.

Metformin treatment and apical GLUT2 location in lean and genetically obese mice. In obese *ob*/*ob* mice and lean *ob*/+ littermates, the impact of metformin on GLUT2 locations in enterocytes was tested. The HOMA-IR value was 38-fold higher in *ob*/*ob* mice than in *ob*/+ mice (Table 2), indicating a strong insulin resistance. In agreement with this finding, insulin concentration at 30 min during the OGTT was ninefold lower in *ob*/+ mice (Table 2).

TABLE 2
Biological parameters of HFLC and *ob*/*ob* and *ob*/+ mice

	Number of mice	Control	HFLC
Weight (g)	12	32.3 ± 0.5	33.0 ± 0.6
Weight gain (g)	12	4.7 ± 0.4	4.6 ± 0.3
GIR (mg · kg^{-1} · min^{-1})	5	31 ± 7	3.5 ± 3.5*
Fasting plasma insulin (mU/L)	5	4.1 ± 0.9	11.0 ± 0.5*
Fasting blood glucose (mmol/L)	5	6.0 ± 0.3	8.0 ± 0.7*
HOMA-IR	5	1.1 ± 0.1	3.9 ± 0.1*
		ob/+	*ob*/*ob*
Weight (g)	8	24.1 ± 0.4	45.4 ± 1.0†
Fasting plasma insulin (mU/L)	5	3.5 ± 0.1	104.0 ± 14.5†
Fasting blood glucose (mmol/L)	5	6.9 ± 0.6	9.1 ± 0.3†
AUC OGTT	8	3.9 ± 0.2	6.4 ± 0.4†
OGTT insulin (mU/L; 30 min)	5	29.6 ± 4.3	136.4 ± 3.2†
HOMA-IR	5	1.1 ± 0.1	41.8 ± 6.5†
HOMA-IR^{met}	5	0.7 ± 0.2	27.0 ± 5.8†

Data are means ± SEM. Bl/6 mice were fed either the M25 control diet or an HFLC diet. Insulin was measured by enzyme-linked immunosorbent assay. HOMA-IR was calculated using the formula [glucose (mmol/L) × insulin (mU/L)/22.5]. HOMA-IR^{met} was measured in mice treated for 10 days with 25 mg/kg metformin twice a day. AUC OGTT, area under curve of blood glucose concentrations after 4 mg/kg oral glucose bolus. Plasma insulin (mU/L) was at 30 min during OGTT. GIR, glucose infusion rate in condition of a hyperinsulinemic-euglycemic clamp after 5 months. *$P < 0.05$. †$P < 0.01$.

As expected in *ob*/+ mice, GLUT2 was only in the basolateral membrane of enterocytes, whereas *ob*/*ob* mice exhibited permanent apical and basolateral GLUT2 (Fig. 4*A*).

Metformin for 10 days in *ob*/*ob* and *ob*/+ mice reduced HOMA-IR values, indicating insulin sensitization. However, *ob*/*ob* mice remained highly insulin resistant (Table 2). In *ob*/+ mice, metformin triggered an apical GLUT2 location despite fasting and high insulin sensitivity (Fig. 4*A*). Accordingly, apical GLUT2 was maintained at a high level in metformin-treated *ob*/*ob* mice (Fig. 4*A*). These results in obese mice link metformin treatment with an apical location of GLUT2.

Functional consequences of apical GLUT2 location on glucose release into the intestinal lumen. When located in the apical and basolateral membranes, GLUT2 should permit bidirectional glucose fluxes down glucose concentration gradients (i.e., absorption from lumen to blood after sugar ingestion and, conversely, efflux from blood to lumen under fasting hyperglycemic conditions). Efflux in freely moving *ob*/*ob* and *ob*/+ mice was explored by intravenous injection of radio-labeled 3-OMG tracer, a nonmetabolizable substrate of the GLUTs. In *ob*/*ob* mice, high blood glucose concentration was maintained by intraperitoneal glucose tolerance test (IPGTT) (1 g/kg; AUC$^{ob/ob}$ 2,047 ± 114 vs. AUC$^{ob/+}$ 1,002 ± 23; $n = 8$). In fasting mice, the intestinal lumen of hyperglycemic *ob*/*ob* mice contained significantly higher glucose amounts than *ob*/+ littermates (after 30 min, 6.9 ± 1 vs. 3.7 ± 0.5 μg · kg^{-1} · min^{-1}; Fig. 4*B*). Moreover, gavage of GLUT2 transport inhibitors (cytochalasin B and phloretin) reduced luminal glucose content by threefold down to *ob*/+ levels, which remained unaffected. This inhibitor-sensitive glucose efflux in *ob*/*ob* mice was estimated to be 3 μg · kg^{-1} · min^{-1}. Thus, permanently apical and basolateral GLUT2 (Fig. 4*A*) can promote glucose release from the intestinal epithelium to the lumen under these conditions.

DISCUSSION

Most morbidly obese subjects (76%) in this study exhibited apical GLUT2 in the fasting state, which contrasted with its basolateral-only location in lean subjects. To the best of our knowledge, this is the first demonstration of an apical GLUT2 location in the human small intestine. We also discovered that GLUT2 could accumulate in the endosomes of 39% obese subjects, thus revealing the complexity of obesity-related adaptation in the intestine.

To understand the underlying mechanisms that alter GLUT2 trafficking in human enterocytes, associations were established between GLUT2 location and the clinical parameters of well-phenotyped obese subjects, such as degree of insulin resistance and unbalanced dietary intake. The correlation between fasting blood glucose concentration and percentage of subjects with apical GLUT2 indicated that this location is linked to changes in glucose homeostasis or diet-induced insulin resistance in humans. Indeed, in hyperglycemic (400 mg/dL) hypoinsulinemic diabetic rats (32) as well as in hyperglycemic (110 mg/dL) hyperinsulinemic mice (14), GLUT2 was observed in the apical membrane of jejunal enterocytes, indicating complex interplay between these parameters to control GLUT2 location. Apical GLUT2 has not been observed in duodenal biopsies from diabetic subjects (21) in contrast to the 73% of obese diabetic subjects displaying apical GLUT2 in the current study. The divergence in results may be related to subject obesity, the intestinal segment studied (duodenum vs. jejunum), or antidiabetic treatments.

The second major observation in 39% of the human obese subjects was the accumulation of GLUT2 in compartments containing the EEA1 endosomal marker. There was a significant association between EEA1/GLUT2 accumulation and HFLC diets. In mice fed an HFLC diet for 5 months (resulting in strong insulin resistance without obesity [14]), we have previously reported apical GLUT2 accumulation in jejunal enterocytes. Prolonged feeding with HFLC for up to 12 months promoted GLUT2 accumulation above the enterocyte nucleus, suggesting that trafficking defaults were further aggravated. Thus, long-term exposure to unbalanced high-fat diets may similarly affect human intestinal function. High-fat diets were reported to alter GLUT2 trafficking in mouse pancreatic β-cells and to promote intracellular GLUT2 location (33). In mouse pancreatic β-cells, high dietary fat was shown to reduce GLUT2 glycosylation from lower GlcNacT-IV transferase (MGAT4a) expression and impaired GLUT2 trafficking into plasma membranes (34). In the current study, MGAT4a protein was reduced twofold in obese subjects exhibiting endosomal versus apical GLUT2. This finding suggests that intestine and pancreatic β-cells share similar mechanisms for glycosylation-related GLUT2 trafficking. In insulin-secreting Min6 cells, high glucose concentration is suspected to trigger GLUT2 degradation in lysosomes (35). In contrast, we did not observe GLUT2 accumulation in lysosomes (LAMP-1) in any of the obese subjects, suggesting that GLUT2 degradation was unaffected. Our findings therefore indicate that macronutrient balance in diet is a controlling factor of GLUT2 trafficking into enterocytes.

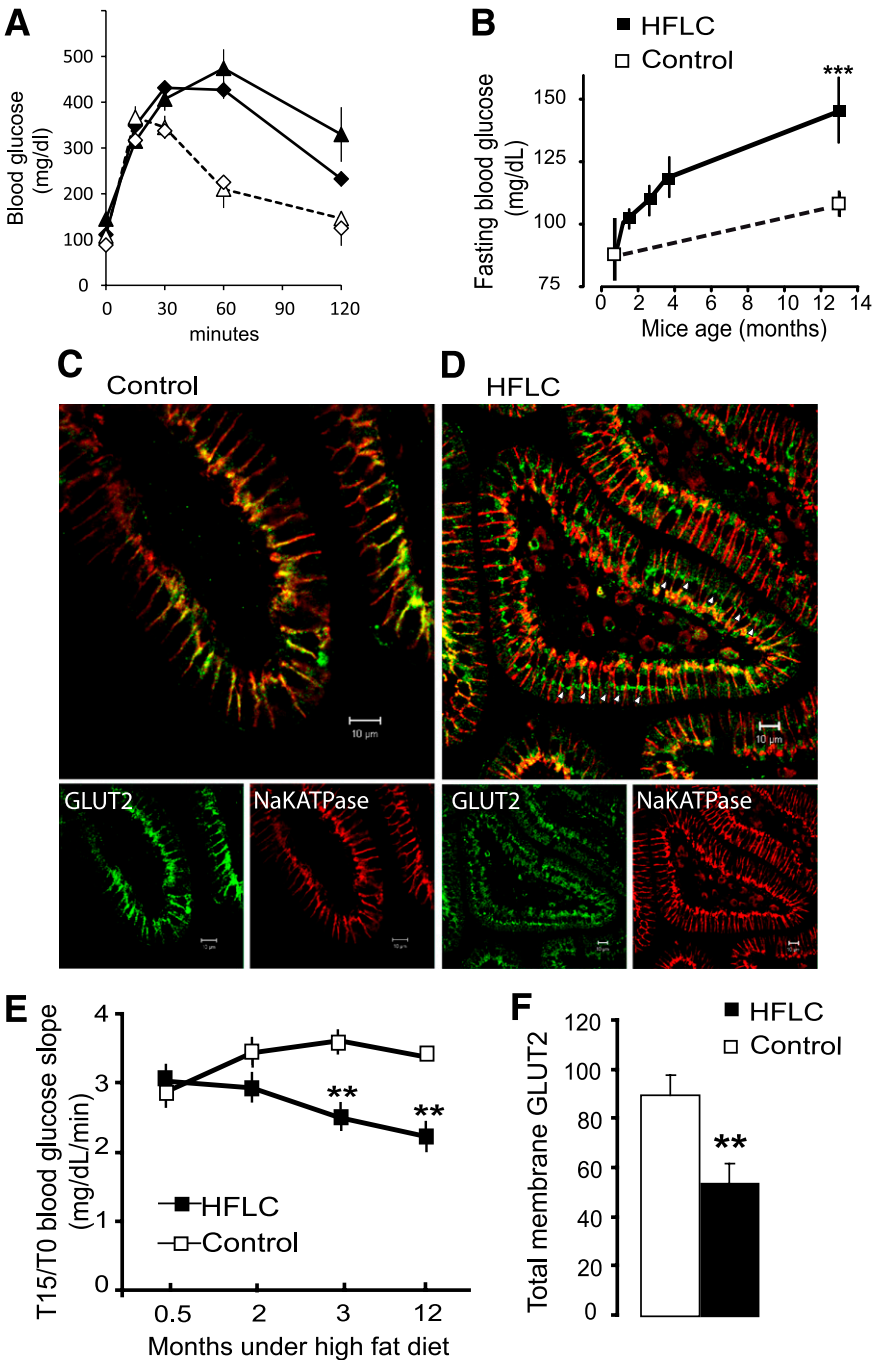

FIG. 3. Endosomal accumulation of GLUT2 in mice fed a high-fat diet. Mice were fed either the control chow diet (M25, *white symbols*) or HFLC diet (*black symbols*) for up to 12 months. *A*: OGTTs are shown after 2 months (*diamonds*) and 12 months (*triangles*) in two groups of eight mice fed the control or HFLC diet. *B*: Fasting blood glucose concentration increases were measured with time (mg/dL ± SEM; $n = 8$; ***$P < 0.001$). *C* and *D*: Representative confocal images of GLUT2 (*green*) and Na,KATPase (*red*) location in 6-μm sections of control and HFLC jejuna after 12 months. Scale 10 μm. Note the endosomal accumulation of GLUT2 (*arrows*) and low basolateral GLUT2 in the jejunum of HFLC-fed mice compared with control diet mice. *E*: Initial slopes (T15/T0) of blood glucose concentration after OGTT ($P < 0.01$) estimating sugar absorption. In *F*, quantification of GLUT2 abundance by Western blot (density arbitrary units ± SEM, **$P < 0.01$) is shown in postnuclear membrane preparations of control and HFLC jejuna. (A high-quality digital representation of this figure is available in the online issue.)**

Metformin, an antidiabetic biguanide drug in current clinical use, promotes a dramatic increase of glucose utilization in human jejunum (36) and in rat intestine (23,37). In rodents, the drug accumulates in the mucosa (38), where it increases SGLT1 and GLUT5 expression, leaving GLUT2 mRNA levels unaltered (24). The effects of metformin on glucose homeostasis have been related to AMPK, increasing glucose utilization, and reducing hepatic glucose output (39). AMPK with 5′-aminoimidazole-4-carboxymide-1-β-D-ribofuranoside (AICAR) recruits GLUT2 in enterocyte apical membranes in rodents (26). This result raises the issue of increasing apical GLUT2 location using pharmacological agents as a means to gain control on intestinal absorption and blood glucose levels. In this study, the 65% of subjects on metformin exhibited apical GLUT2, suggesting that the drug may also modify intestinal sugar transepithelial

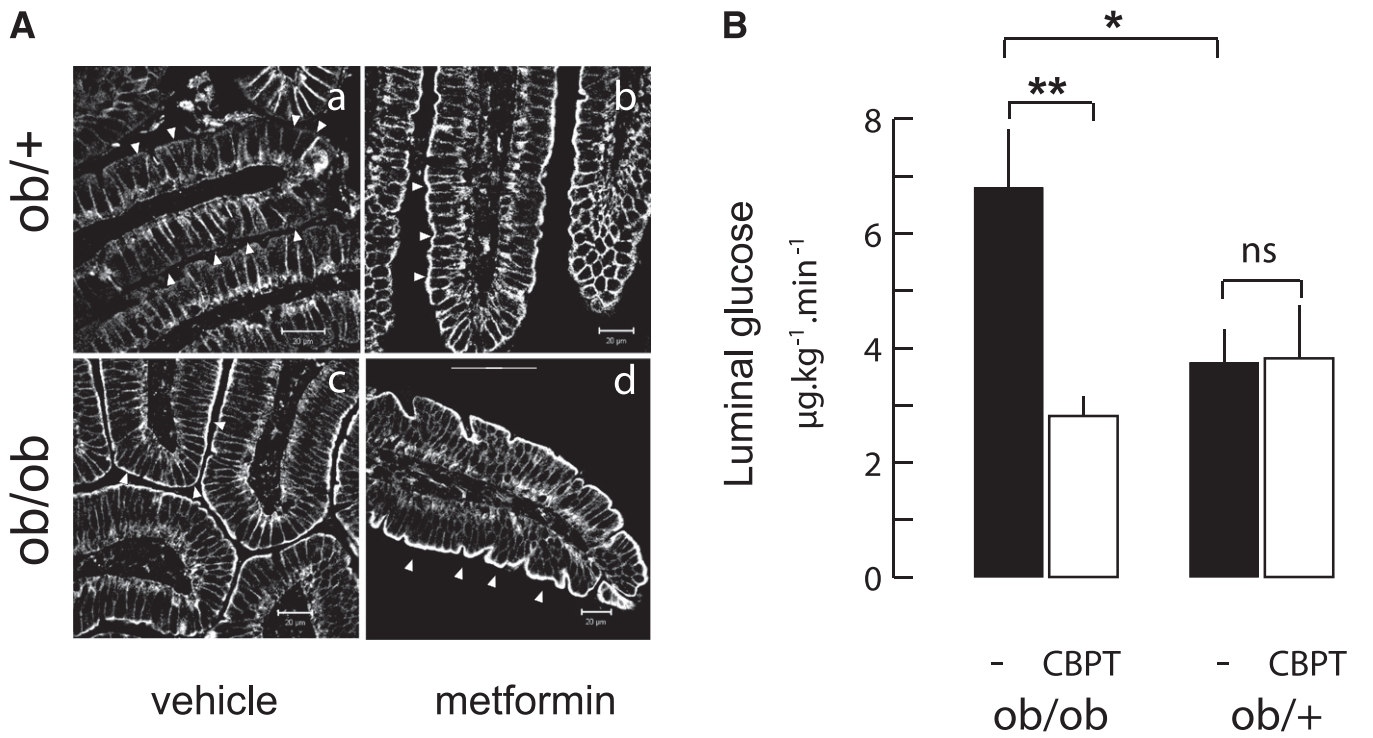

FIG. 4. Apical GLUT2 increase after metformin treatment and the functional significance in obese mice. *A*: *ob/ob* mice fed a standard diet (M25) received either the H_2O vehicle or 25 mg/kg metformin twice a day for 10 days. Representative confocal images of GLUT2 location in jejuna from fasted *ob/+* (*upper row*) and *ob/ob* (*lower row*) mice after treatment with vehicle (*left column*) or metformin (*right column*) are shown. *Arrowheads* indicate the apical side of enterocytes. Scale 10 µm. *B*: Release of glucose in the luminal content of freely moving *ob/ob* and *ob/+* mice measured 30 min after an intravenous injection of radioactive 3-OMG tracer. Mice were fasted overnight and received 1 g/kg glucose by intraperitoneal injection. Before tracer injection, half of the mice also received by gavage an oral bolus of ethanolic water (1/1,000, vol/vol) containing cytochalasin B (0.3 mmol/L) and phloretin (1 mmol/L) (CBPT, □) or vehicle (■). Data are expressed as $\mu g \cdot kg^{-1} \cdot min^{-1} \pm$ SEM. Controls ($n = 8$) and CBPT ($n = 4$) per phenotype are shown. *$P < 0.05$, **$P < 0.01$.

fluxes. However, a study to address the multiple associations of antidiabetic drugs on intestinal GLUT2 location requires a large number of diabetic subjects.

The harm or benefits of apical GLUT2 location is schematized in Fig. 5. Under fasting conditions, SGLT1 captures any trace glucose from the lumen. GLUT2 in the basolateral membrane provides a glucose entry pathway to fulfill enterocyte metabolic needs. We showed that the transient insertion of apical GLUT2 in healthy enterocytes, occurring after a sugar-rich meal, triples the initial rate of sugar uptake (10). The magnitude of postprandial hyperglycemia caused by rapid entry of sugar into the bloodstream will modulate pancreatic insulin secretion. The action of insulin will then contribute to internalize apical GLUT2 and promote a return to basal location and function (14). We showed in mouse that pathological and permanent apical GLUT2 in obesity favors glucose release from the mucosa into the lumen. Glucose efflux mediated by permanent apical GLUT2 will occur as soon as the glucose gradient between blood and lumen is reversed. This efflux into the lumen will maintain an abnormal glucose provision to fuel bacteria metabolism. This result may contribute to changes in gut microbiota, as observed in obese mice (40). We anticipate that permanent apical GLUT2 accelerates glucose uptake immediately after a sugar-rich meal in obese subjects as well as in lean subjects. The consequences of permanent apical GLUT2 on the net intestinal sugar absorption need to be quantified in more detail.

GLUT2 trafficking in cell types other than enterocyte and kidney cells is not fully understood. In the rat liver, GLUT2 and insulin receptors are internalized as a complex that was proposed as a means to accelerate insulin inhibition of hepatic glucose production (41). In rodent pancreatic β-cells, GLUT2 location depends on the abundance of glucose in the diet (34) or in the culture medium of cell lines (35) and could modulate insulin secretion. In the mouse brain, GLUT2 is involved in the regulation of food intake (42,43). A coordinated regulation of GLUT2 trafficking in these tissues might implement a gut-brain axis control on glucose homeostasis.

Our study reveals that GLUT2 can be inserted into the apical membrane of human enterocytes. In morbidly obese subjects, GLUT2 accumulated in apical and endosomal membranes. These pathological locations have been respectively linked to metabolic alteration and nutritional patterns. Transepithelial glucose exchange is favored by apical GLUT2 and reduced by endosomal GLUT2. Apical GLUT2 could be triggered by drugs such as metformin to provide a glucose exit pathway into the lumen contributing to the drug hypoglycemic effect. Apical GLUT2 can therefore provide plasticity to sugar absorption and constitute a compensatory/adaptive mechanism to limit the magnitude of hyperglycemia. Altered GLUT2 locations in enterocyte are a sign of intestinal adaptation to human metabolic pathology.

ACKNOWLEDGMENTS

The work was supported by Institut National de la Santé et de la Recherche Médicale (INSERM), Pierre and Marie Curie (UMPC) P6 and René Descartes P5 universities, and

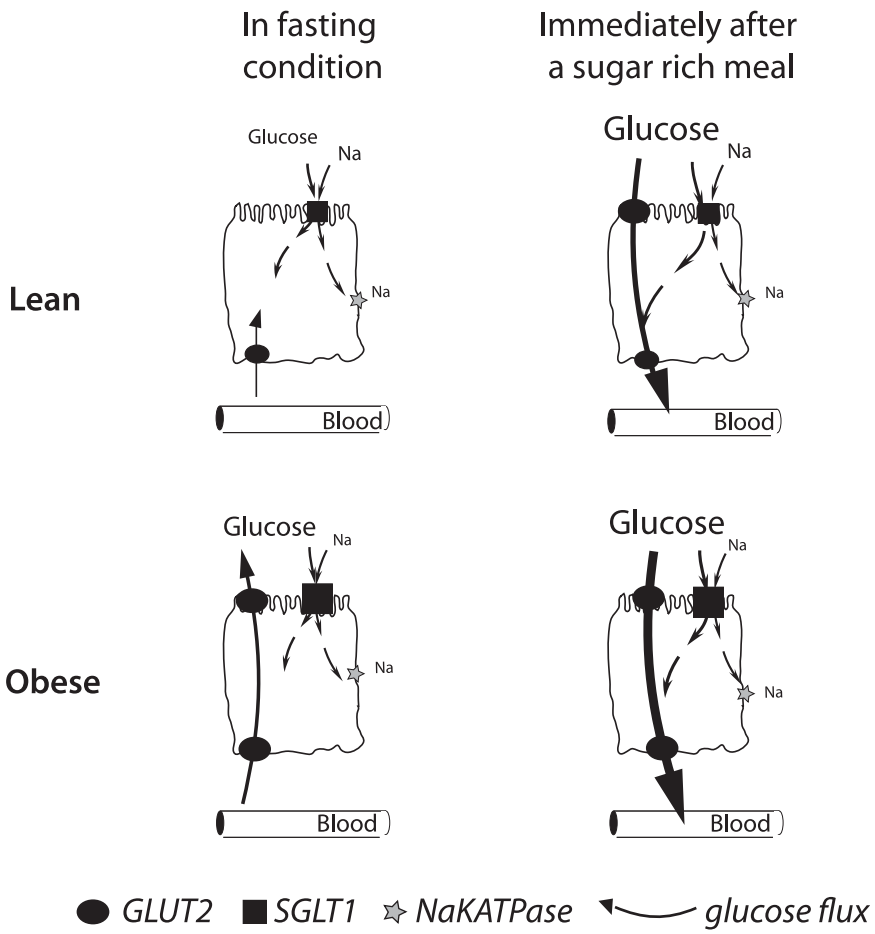

FIG. 5. Roles of apical GLUT2 in health and metabolic disease glucose absorption and secretion related to apical GLUT2 location in enterocytes depend on the glucose concentration difference between blood and lumen. In fasting lean subjects (*first line schemes*), glucose fluxes across epithelial cells occur via SGLT1 in the apical membrane and exit via basolateral GLUT2. Immediately after a sugar-rich meal, GLUT2 is rapidly and transiently inserted in apical membranes to increase glucose absorption (*thick black arrow*), thereby complementing SGLT1 uptake. Obese subjects (*second line*) are characterized by permanent apical GLUT2. Fasting hyperglycemia can therefore mediate a blood-to-lumen glucose flux, i.e., secretion through enterocytes into the intestinal lumen. In contrast, after a sugar-rich meal, permanent apical GLUT2 instantly provides a large uptake of glucose. This absorption pathway for glucose remains to be measured.

the Centre National de la Recherche Scientifique (CNRS). A.C. and J.G. hold postdoctoral fellowships from Agence Nationale de la Recherche-Alimentation et Industries Alimentaires (ANR-ALIA 007-01).

No potential conflicts of interest relevant to this article were reported.

A.A.-O., M.M.-S., and K.G. performed the immunolocalizations. C.P., A.C., and J.T. recruited subjects and performed the phenotype and statistical analysis. N.V. and D.H. did tissue sampling and processing. D.C. was in charge of electron microscopy and supervised K. Bourhaba. M.L.G., A.H., and P.S. contributed to biochemical studies in mouse and human intestines. J.G., A.La., and C.M. performed in vivo glucose efflux measures. K.C. supervised clinical studies and statistical analysis and contributed to the writing of the manuscript. A.Le. and E.B.-L. initiated the study, designed experiments, supervised the analysis, and wrote the manuscript.

Part of this work was presented at the Physiological Society Themed Meeting, Newcastle upon Tyne, U.K., 6–8 September 2009 and Epithelium and Membrane Transport Group, Salerno, Italy, 7–10 April 2010.

The authors thank Assistance Publique-Hôpitaux de Paris and Direction of Clinical Research, which promoted and supported clinical investigations. The authors thank the following individuals who helped to provide the raw data and tissue samples: Dr. D. Lamarque (Hotel Dieu Hospital Assistance Publique-Hôpitaux de Paris, Paris) for double balloon endoscopy, animal house personnel, and C. Lasne (Centre d'Exploration Fonctionnelle, INSERM/UPMC unit UMRS 872) for the OGTT in mice; C. Klein and the imaging core facility of CRC (Centre d'Imagerie Cellulaire et Cytometrie, UMRS 872, Paris); A. Benkouhi for enzyme-linked immunosorbent assays (CRC-UMRS 872, team 9); C. Baudouin and F. Marchelli for subject recruitment and data collection at the Centre de Recherche en Nutrition Humaine (CRNH), Pitié-Salpêtrière Hospital, Reference Center for Medical and Surgical Care of Obesity (CRMO); and S. Gougis for dietary evaluation at CRMO. The authors also thank Jerome Brooks, PhD, Alex Edelman and Associates, Malakof, France (www.edelman.com), for the final editing of the manuscript.

REFERENCES

1. Drozdowski L, Thomson AB. Intestinal hormones and growth factors: effects on the small intestine. World J Gastroenterol 2009;15:385–406
2. Wright EM, Hirayama BA, Loo DF. Active sugar transport in health and disease. J Intern Med 2007;261:32–43

3. Chaikomin R, Doran S, Jones KL, et al. Initially more rapid small intestinal glucose delivery increases plasma insulin, GIP, and GLP-1 but does not improve overall glycemia in healthy subjects. Am J Physiol Endocrinol Metab 2005;289:E504–E507
4. Raybould HE. Nutrient sensing in the gastrointestinal tract: possible role for nutrient transporters. J Physiol Biochem 2008;64:349–356
5. Burant CF, Takeda J, Brot-Laroche E, Bell GI, Davidson NO. Fructose transporter in human spermatozoa and small intestine is GLUT5. J Biol Chem 1992;267:14523–14526
6. Thorens B. Glucose transporters in the regulation of intestinal, renal, and liver glucose fluxes. Am J Physiol 1996;270:G541–G553
7. Cheeseman CI, Maenz DD. Rapid regulation of D-glucose transport in basolateral membrane of rat jejunum. Am J Physiol 1989;256:G878–G883
8. Cheeseman C. GLUT7: a new intestinal facilitated hexose transporter. Am J Physiol Endocrinol Metab 2008;295:E238–E241
9. Kellett GL, Helliwell PA. The diffusive component of intestinal glucose absorption is mediated by the glucose-induced recruitment of GLUT2 to the brush-border membrane. Biochem J 2000;350:155–162
10. Gouyon F, Caillaud L, Carriere V, et al. Simple-sugar meals target GLUT2 at enterocyte apical membranes to improve sugar absorption: a study in GLUT2-null mice. J Physiol 2003;552:823–832
11. Habold C, Foltzer-Jourdainne C, Le Maho Y, Lignot JH, Oudart H. Intestinal gluconeogenesis and glucose transport according to body fuel availability in rats. J Physiol 2005;566:575–586
12. Kellett GL, Brot-Laroche E, Mace OJ, Leturque A. Sugar absorption in the intestine: the role of GLUT2. Annu Rev Nutr 2008;28:35–54
13. Kellett GL, Brot-Laroche E. Apical GLUT2: a major pathway of intestinal sugar absorption. Diabetes 2005;54:3056–3062
14. Tobin V, Le Gall M, Fioramonti X, et al. Insulin internalizes GLUT2 in the enterocytes of healthy but not insulin-resistant mice. Diabetes 2008;57:555–562
15. Kwon O, Eck P, Chen S, et al. Inhibition of the intestinal glucose transporter GLUT2 by flavonoids. FASEB J 2007;21:366–377
16. Burant CF, Flink S, DePaoli AM, et al. Small intestine hexose transport in experimental diabetes: increased transporter mRNA and protein expression in enterocytes. J Clin Invest 1994;93:578–585
17. Kahn BB, Flier JS. Obesity and insulin resistance. J Clin Invest 2000;106:473–481
18. Kahn SE, Hull RL, Utzschneider KM. Mechanisms linking obesity to insulin resistance and type 2 diabetes. Nature 2006;444:840–846
19. Saberi M, Woods NB, de Luca C, et al. Hematopoietic cell-specific deletion of toll-like receptor 4 ameliorates hepatic and adipose tissue insulin resistance in high-fat-fed mice. Cell Metab 2009;10:419–429
20. Bailey CJ. Insulin resistance and antidiabetic drugs. Biochem Pharmacol 1999;58:1511–1520
21. Dyer J, Wood IS, Palejwala A, Ellis A, Shirazi-Beechey SP. Expression of monosaccharide transporters in intestine of diabetic humans. Am J Physiol Gastrointest Liver Physiol 2002;282:G241–G248
22. Bailey CJ, Wilcock C, Day C. Effect of metformin on glucose metabolism in the splanchnic bed. Br J Pharmacol 1992;105:1009–1013
23. Pénicaud L, Hitier Y, Ferré P, Girard J. Hypoglycaemic effect of metformin in genetically obese (fa/fa) rats results from an increased utilization of blood glucose by intestine. Biochem J 1989;262:881–885
24. Lenzen S, Lortz S, Tiedge M. Effect of metformin on SGLT1, GLUT2, and GLUT5 hexose transporter gene expression in small intestine from rats. Biochem Pharmacol 1996;51:893–896
25. Ikeda T, Iwata K, Murakami H. Inhibitory effect of metformin on intestinal glucose absorption in the perfused rat intestine. Biochem Pharmacol 2000;59:887–890
26. Walker J, Jijon HB, Diaz H, Salehi P, Churchill T, Madsen KL. 5-Aminoimidazole-4-carboxamide riboside (AICAR) enhances GLUT2-dependent jejunal glucose transport: a possible role for AMPK. Biochem J 2005;385:485–491
27. Sjöström L, Lindroos AK, Peltonen M, et al. Lifestyle, diabetes, and cardiovascular risk factors 10 years after bariatric surgery. N Engl J Med 2004;351:2683–2693
28. Burcelin R, Crivelli V, Dacosta A, Roy-Tirelli A, Thorens B. Heterogeneous metabolic adaptation of C57BL/6J mice to high-fat diet. Am J Physiol Endocrinol Metab 2002;282:E834–E842
29. Lee S, Muniyappa R, Yan X, et al. Comparison between surrogate indexes of insulin sensitivity and resistance and hyperinsulinemic euglycemic clamp estimates in mice. Am J Physiol Endocrinol Metab 2008;294:E261–E270
30. Affleck JA, Helliwell PA, Kellett GL. Immunocytochemical detection of GLUT2 at the rat intestinal brush-border membrane. J Histochem Cytochem 2003;51:1567–1574
31. Brot-Laroche E, Dao MT, Alcalde AI, Delhomme B, Triadou N, Alvarado F. Independent modulation by food supply of two distinct sodium-activated D-glucose transport systems in the guinea pig jejunal brush-border membrane. Proc Natl Acad Sci U S A 1988;85:6370–6373
32. Corpe CP, Basaleh MM, Affleck J, Gould G, Jess TJ, Kellett GL. The regulation of GLUT5 and GLUT2 activity in the adaptation of intestinal brush-border fructose transport in diabetes. Pflugers Arch 1996;432:192–201
33. Reimer MK, Ahrén B. Altered beta-cell distribution of pdx-1 and GLUT-2 after a short-term challenge with a high-fat diet in C57BL/6J mice. Diabetes 2002;51(Suppl. 1):S138–S143
34. Ohtsubo K, Takamatsu S, Minowa MT, Yoshida A, Takeuchi M, Marth JD. Dietary and genetic control of glucose transporter 2 glycosylation promotes insulin secretion in suppressing diabetes. Cell 2005;123:1307–1321
35. Hou JC, Williams D, Vicogne J, Pessin JE. The glucose transporter 2 undergoes plasma membrane endocytosis and lysosomal degradation in a secretagogue-dependent manner. Endocrinology 2009;150:4056–4064
36. Bailey CJ, Wilcock C, Scarpello JH. Metformin and the intestine. Diabetologia 2008;51:1552–1553
37. Bailey CJ, Mynett KJ, Page T. Importance of the intestine as a site of metformin-stimulated glucose utilization. Br J Pharmacol 1994;112:671–675
38. Wilcock C, Bailey CJ. Accumulation of metformin by tissues of the normal and diabetic mouse. Xenobiotica 1994;24:49–57
39. Zhou G, Myers R, Li Y, et al. Role of AMP-activated protein kinase in mechanism of metformin action. J Clin Invest 2001;108:1167–1174
40. Turnbaugh PJ, Ley RE, Mahowald MA, Magrini V, Mardis ER, Gordon JI. An obesity-associated gut microbiome with increased capacity for energy harvest. Nature 2006;444:1027–1031
41. Eisenberg ML, Maker AV, Slezak LA, et al. Insulin receptor (IR) and glucose transporter 2 (GLUT2) proteins form a complex on the rat hepatocyte membrane. Cell Physiol Biochem 2005;15:51–58
42. Bady I, Marty N, Dallaporta M, et al. Evidence from glut2-null mice that glucose is a critical physiological regulator of feeding. Diabetes 2006;55:988–995
43. Stolarczyk E, Guissard C, Michau A, et al. Detection of extracellular glucose by GLUT2 contributes to hypothalamic control of food intake. Am J Physiol Endocrinol Metab 2010;298:E1078–E1087